

Early Divergence in Misfolding Pathways of Amyloid-Beta Peptides

Salvatore Mamone,^[a, d] Stefan Glöggler,^[a, d] Stefan Becker,^[a] and Nasrollah Rezaei-Ghaleh^{*[a, b, c]}

The amyloid cascade hypothesis proposes that amyloid-beta ($A\beta$) aggregation is the initial triggering event in Alzheimer's disease. Here, we utilize NMR spectroscopy and monitor the structural dynamics of two variants of $A\beta$, $A\beta_{40}$ and $A\beta_{42}$, as a function of temperature. Despite having identical amino acid sequence except for the two additional C-terminal residues, $A\beta_{42}$ has higher aggregation propensity than $A\beta_{40}$. As revealed by the NMR data on dynamics, including backbone chemical shifts, intra-methyl cross-correlated relaxation rates and glycine-based singlet-states, the C-terminal region of $A\beta$, especially the G33-L34-M35 segment, plays a particular role in the early steps of temperature-induced $A\beta$ aggregation. In $A\beta_{42}$, the distinct dynamical behaviour of C-terminal residues at higher temperatures is accompanied with marked changes in the backbone dynamics of residues V24-K28. The distinctive role of the C-terminal region of $A\beta_{42}$ in the initiation of aggregation defines a target for the rational design of $A\beta_{42}$ aggregation inhibitors.

Amyloid-beta peptides ($A\beta$) are the main constituents of senile plaques in the brains of Alzheimer's disease (AD) patients.^[1,2] Several lines of evidence suggest a crucial role for $A\beta$ aggregation as the initial triggering event in AD pathology.^[1] Consequently, $A\beta$ aggregation is widely considered as an ideal target for anti-AD drug development.

The two common variants of $A\beta$ are $A\beta_{1-40}$ ($A\beta_{40}$) and $A\beta_{1-42}$ ($A\beta_{42}$), which are identical in the amino acid sequence except for the two additional C-terminal residues in $A\beta_{42}$ (Figure 1A).^[2] Despite being similarly unstructured in the monomeric state,^[3] $A\beta_{42}$ is more aggregation prone and neurotoxic than $A\beta_{40}$.^[1] Early studies of $A\beta$ aggregation suggest that the C-terminus of $A\beta$ plays a key role in amyloidogenesis and that the oligomeric assembly of $A\beta_{40}$ and $A\beta_{42}$ proceeds through distinct pathways.^[4,5] The $A\beta_{42}$ was shown to be more rigid than $A\beta_{40}$ at the C-terminus,^[6] probably due to the transient formation of a β -sheet structure in $A\beta_{42}$.^[7] In recent years, several structural models of $A\beta_{40}$ and $A\beta_{42}$ fibrils have been published, providing clear evidence for their differences in the fibril state.^[8–11] In addition, structural models of the intermediate $A\beta$ aggregates implicate that $A\beta_{42}$ oligomers are structurally distinct in the C-terminal region.^[12]

The rational design of an $A\beta$ aggregation inhibitor ideally requires a mechanistic understanding of the early stages of aggregation before any toxic $A\beta$ species is formed. Solution-state NMR spectroscopy allows monitoring early events during $A\beta$ aggregation at atomic resolution. Here, we utilize this technique to probe the backbone and sidechain dynamics of

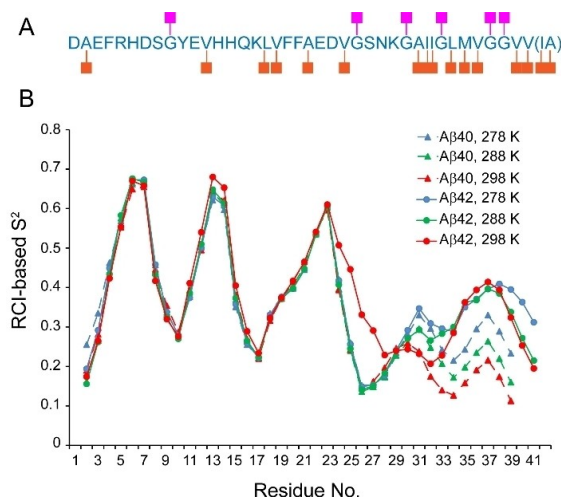


Figure 1. A. Amino-acid sequence of $A\beta_{1-40(42)}$, showing the sequence distribution of glycine (purple squares) and methyl-containing (orange squares) residues. B) Temperature-dependence of backbone dynamics in $A\beta_{40}$ and $A\beta_{42}$. Residue-specific squared order parameters (S^2) of $A\beta_{40}$ and $A\beta_{42}$ in dependence of temperature, based on the Random Coil Index (RCI) values derived from backbone chemical shifts, are shown. Note the differences between $A\beta_{40}$ and $A\beta_{42}$, in particular from residue V24 towards the C-terminus. See Tables S1 and S2 for residue-specific chemical shifts, esp. with regard to residues with missing assignments.

[a] Dr. S. Mamone, Dr. S. Glöggler, Dr. S. Becker, Dr. N. Rezaei-Ghaleh

Department for NMR-based Structural Biology
Max Planck Institute for Biophysical Chemistry
Am Faßberg 11, 37077 Göttingen, Germany

[b] Dr. N. Rezaei-Ghaleh

Department of Neurology,
University Medical Center Göttingen
Waldweg 33, 37073 Göttingen, Germany

[c] Dr. N. Rezaei-Ghaleh

Institute of Physical Biology,
Heinrich Heine University Düsseldorf
Universitätsstraße 1, 40225 Düsseldorf, Germany
E-mail: Nasrollah.Rezaei.Ghaleh@hhu.de

[d] Dr. S. Mamone, Dr. S. Glöggler

Center for Biostructural Imaging of Neurodegeneration
University Medical Center Göttingen
Von-Siebold-Str. 3A, 37075 Göttingen, Germany

Supporting information for this article is available on the WWW under <https://doi.org/10.1002/cphc.202100542>

© 2021 The Authors. ChemPhysChem published by Wiley-VCH GmbH. This is an open access article under the terms of the Creative Commons Attribution Non-Commercial NoDerivs License, which permits use and distribution in any medium, provided the original work is properly cited, the use is non-commercial and no modifications or adaptations are made.

A β 40 and A β 42 and exploiting them as local proxies of aggregation-related events (Figure 1A), we provide evidence for the early divergence of the misfolding pathways of A β 40 and A β 42.

NMR chemical shifts are sensitive probes of conformational dynamics of proteins at pico-to-microseconds.^[13] To monitor the backbone dynamics of A β in dependence of temperature, we measured the backbone (HN, HA, N, CA, CO) chemical shifts of A β 40 and A β 42 at three temperatures of 278, 288 and 298 K (SI, Tables S1 and S2). We then followed the random coil index (RCI)-based order parameters (S^2) approach of ref.,^[14] which in intrinsically disordered proteins (IDPs) represents the conformational heterogeneity of their ensembles and therefore enables “qualitative” monitoring of temperature effects on A β 's backbone dynamics. As shown in Figure 1B, the increase in temperature altered the structural dynamics of A β 40 and A β 42 in two different ways: in A β 40, increasing the temperature from 278 to 288 and then 298 K had little impact on the backbone mobility of residues proximal to G29, while the backbone mobility of residues A30 towards the C-terminus was clearly enhanced. In A β 42, up to residue D23, the temperature dependence of mobility was almost the same as that of A β 40. However, sharp differences were observed from residue V24 onwards; residues V24–K28 became more rigid at higher temperatures, residues G29 and L34–G38 retained their mobility, and only residues A30–G33 and to lesser extent V39–I41 got more mobile at higher temperatures. The distinctive dynamical behavior of the C-terminal region of A β 42 is in qualitative agreement with the ¹⁵N relaxation-based reports of A β 's ps–ns dynamics,^[6] although a quantitative comparison of the ¹⁵N relaxation- and RCI-based S^2 is not possible.

Next, to investigate the temperature-dependent changes in the side-chain dynamics of A β 40 and A β 42, the ¹³C,¹H HSQC spectra were measured for the methyl (CH₃) groups of alanine, valine, leucine, isoleucine and methionine residues (SI, Figure S1). As suggested by the structural models of A β 40 and A β 42 fibrils,^[8–11] these hydrophobic residues play significant roles in the stability of A β aggregates. Hydrophobic interactions are strongly temperature-dependent and their destabilization at very low or high temperatures promotes dissociation of amyloid fibrils.^[15] The temperature-induced perturbations in chemical shifts were overall similar for A β 40 and A β 42, however, the C-terminal residues, I41 and A42, of A β 42 showed a relatively large chemical shift change (Figure 2). The ¹³C and ¹H chemical shifts did not show any significant A β concentration dependence (SI, Figure S2), suggesting that their temperature variation reflected A β 's conformational dynamics predominantly in the monomeric state. In both A β 40 and A β 42, the methyl groups exhibited large variation in temperature dependence of their peak intensity (SI, Figures S3 and S4). Interestingly, in both A β 40 and A β 42, the most prominent intensity reduction was observed for the methyl group of M35. Less prominent albeit considerable intensity loss was observed for the methyl groups of L34, V40 and V39 in A β 40 (SI, Figure S3), and those of A42, V36/V39, L34, L17 and V18 in A β 42 (SI, Figure S4). In A β 42, all the methyl groups showed an intensity drop at 302 K, as a consequence of aggregation-induced monomer loss.

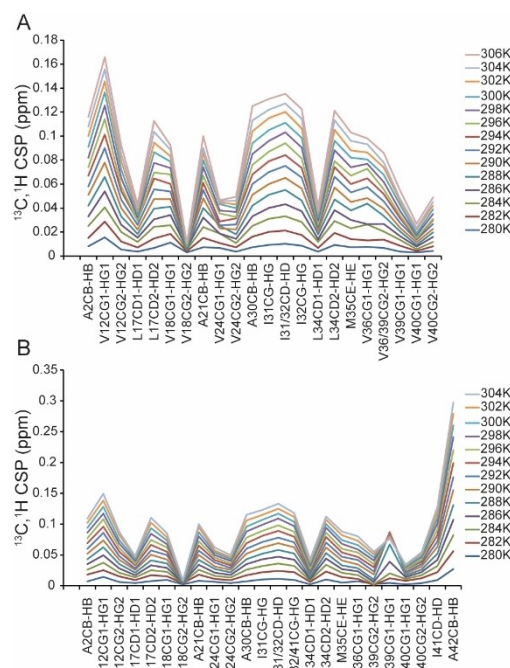


Figure 2. Combined ¹³C and ¹H chemical shift perturbation (CSP) of the methyl groups of A β 40 (A) and A β 42 (B) upon temperature rise, evaluated with respect to the chemical shifts obtained at 278 K. Note that the C-terminal methyl groups of A β 42 (of I41 and A42) exhibit a relatively large CSP in dependence of temperature.

To further investigate the effect of temperature on methyl dynamics in A β 40 and A β 42, the cross-correlated relaxation (CCR, Γ) rates between three ¹³C,¹H dipolar couplings of the methyl groups were measured through constant-time ¹H-coupled ¹³C,¹H HSQC spectra from the intensities of different peaks in the quartet, as described in Ref. [16] (Figure 3). The methyl CCR rates report the reorientational mobility of the three-fold symmetry axis of the methyl groups.^[16,17] In A β 40, the CCR rates of most of the methyl groups decreased by temperature, in accord with the temperature-dependent decrease in viscosity/temperature (η/T) ratios and its resultant enhancement in side-chain mobility (SI, Table S2). However, the methyl groups of L17, L34, M35 and V40 showed an unexpected increase in the CCR rates at 310 K, indicating their significantly lower mobility at this temperature (Figure 4A). In comparison, in A β 42, the methyl groups of L17 obeyed the general trend of mobility enhancement upon temperature increase up to 298 K, but the methyl groups of L34, V40 and A42 followed an opposite trend and became relatively rigid at 298 K (Figure 4B and SI, Table S3).

A β contains six glycine residues, G9, G25, G29, G33, G37 and G38. To utilize glycines as local probes of structural dynamics of A β during aggregation, we monitored glycines of A β 40 and A β 42 through a singlet-filtered NMR method.^[18] Singlet-states are effective spin-0 states formed in homonuclear spin-1/2 pairs and can be detected only indirectly.^[19,20] The singlet-states have been previously utilized for monitoring protein conformational and dynamical changes during unfolding.^[21,22] Glycines have a

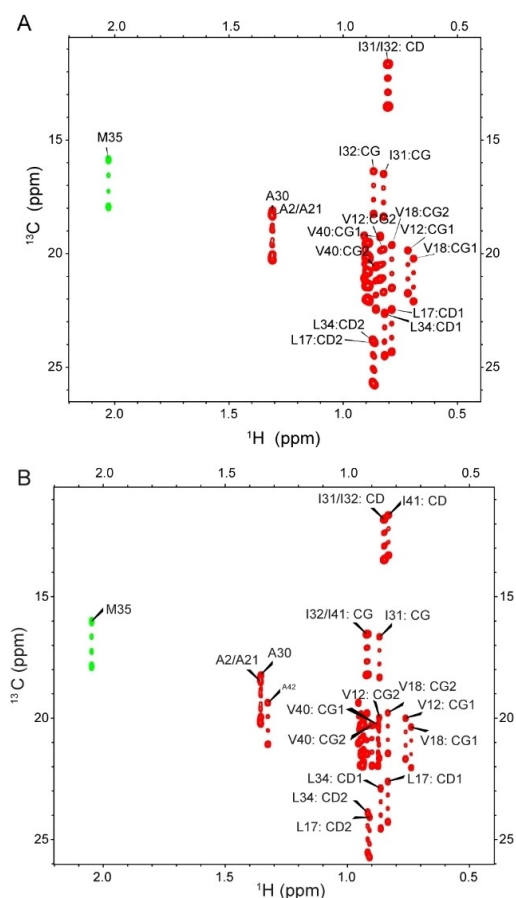


Figure 3. ^1H -coupled constant-time ^{13}C , ^1H HSQC spectrum of A β 40 (A) and A β 42 (B) in the methyl region measured at 273 K, used for the determination of methyl cross-correlated relaxation (CCR, Γ) rates. The green peaks belong to Met35, which are 180-degree out-of-phase with respect to the other methyl groups shown in red. The phase difference is caused by the evolution of C–C coupling in all but methionine’s methyl groups.

pair of HA spins, which in deuterated solvents become largely isolated from all other protons. Since the HA pairs of the six glycines of A β experience different coupling regimes (depending on the ratio between their chemical shift difference, $\Delta\omega$, and the 2J scalar coupling between them), they could be monitored selectively through the gc-M2S sequence (Figure 5 and SI, Figure S5).^[18] The singlet-filtered approach is particularly advantageous in A β where the peaks of glycine residues in proton-based homonuclear NMR spectra are not well resolved.

In A β 40, the G25 and to a lower extent G29, G37, G38 and G9 residues showed an initial increase in the intensity upon heating, followed by the intensity loss at higher temperatures (Figure 6A). The G33 residue however obeyed an opposite trend: its intensity decreased up to 288 K, then increased by further heating up to 310 K. The distinction between G33 and other glycine residues became more pronounced in A β 42: upon heating to 293 K, the G33 residue showed an intensity gain by a factor of ~ 2 , while the other glycine residues kept (G25) or lost (G29, G38, G9 and G37) their intensity (Figure 6B). Notably, in A β 40 and especially in A β 42 the intensity gain of G33 were

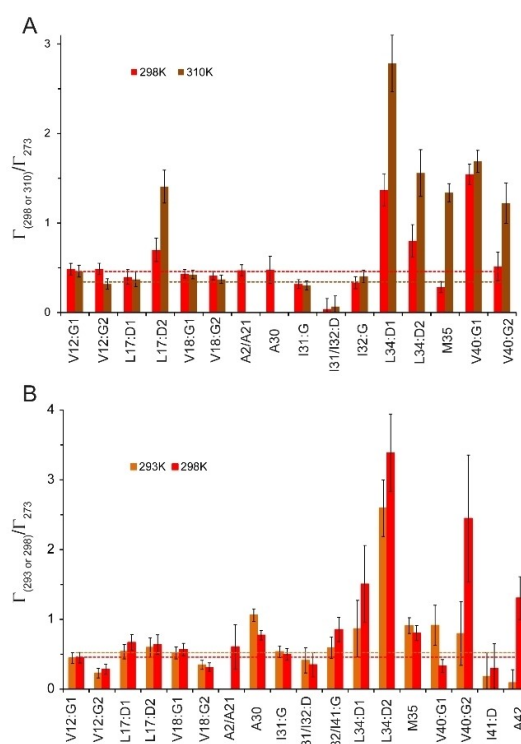


Figure 4. Temperature dependence of methyl dynamics in A β 40 and A β 42, reported as the ratio of methyl cross-correlated relaxation (CCR, Γ) rates obtained at different temperatures. The dashed line represents the viscosity/temperature (η/T) ratio at different temperatures. Most methyl groups experience larger mobility at higher temperatures (hence smaller Γ rates), comparable to what would be expected from the η/T ratio. Note that in A β 40 (A), L17, L34, M35 and V40, and in A β 42 (B), L34, V40 and A42 follow an opposite trend and become relatively rigid.

accompanied by temperature-induced A β monomer loss due to aggregation.

Subsequently, we measured the singlet-state (T_s) and spin-lattice relaxation times (T_1) of A β ’s glycines at different temperatures. There are three distinct dynamical regimes in peptide-based singlet-states: fast, intermediate, and slow. In “fast” and “slow” regimes, the T_s and T_1 change in the same direction when the rotational correlation time (τ_c) is altered, while in the “intermediate” regime, they change in the opposite directions.^[23] Consequently, the T_s/T_1 ratio exhibits its largest sensitivity to dynamical changes in the intermediate regime. Due to the relatively low sensitivity and long duration of the singlet-state NMR experiments, these relaxation measurements were performed only for the less aggregation-prone A β 40. As shown in SI, Figures S6 and S7, all glycine residues of A β 40 except G33 showed slight temperature-dependent increase in T_s and decrease in T_1 at temperatures above 281 K, which considering their τ_c being greater than $1/\omega_H \sim 230$ ps,^[24] suggests their relative mobilization in the intermediate regime.^[23] Unlike them, the G33 residue seems to have undergone a relative rigidification in the same temperature range. When the T_s/T_1 ratio was plotted against the temperature, the distinct behavior of the G33 residue became more evident (Figure 6 and SI, Figure S8). Overall, the singlet-state intensity (and

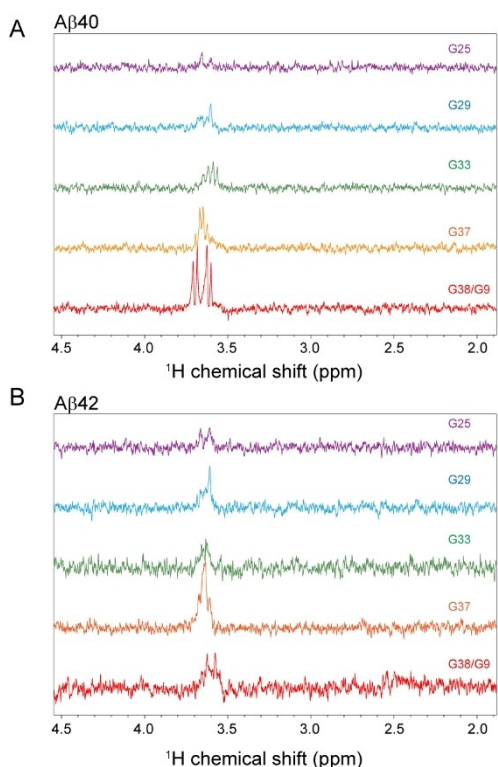


Figure 5. The singlet-filtered 1D ^1H spectra of A β 40 (A) and A β 42 (B) for different glycines. All the six glycine residues of A β 40 and A β 42 could be detected. Since the $\Delta\omega/J$ ratios of G9 and G38 are similar, their singlet-states could not be separated. The spectra were obtained in A β solutions in 100% D_2O at 278 K.

relaxation) data point to a particular role of G33 in temperature-induced initiation of A β aggregation.

To investigate whether the temperature-induced alterations in the conformational dynamics of A β are due to intramolecular changes in A β monomers or alternatively caused by the formation of A β oligomers in rapid exchange with NMR-visible monomers, we measured the hydrodynamic radii (R_h) of A β 40 and A β 42 through NMR diffusion experiments. At 278 K, the R_h of A β 40 and A β 42 were 2.0 ± 0.1 and 2.1 ± 0.1 nm, respectively, consistent with the predominantly monomeric state of NMR-visible A β peptides. Upon temperature increase to 288 and 298 K, the R_h of A β 40 remained unchanged, while the R_h of A β 42 showed slight reduction to 2.0 ± 0.2 and 1.8 ± 0.2 nm, respectively. The slight reduction of the R_h of A β 42 at 298 K occurred despite significant ($\sim 75\%$) monomer loss due to aggregation, indicating that the exchange between A β 42 monomers and oligomers is slow in the diffusion timescale. It is notable that our diffusion data does not exclude the weak interaction between A β monomers and stable high-molecular-weight A β aggregates, as shown previously.^[25] However, in the present study, we have avoided the experimental conditions, e.g. high A β concentrations, which induce the formation of protofibrils or other large aggregates. Overall, in line with the lack of concentration dependence of NMR chemical shifts (SI, Figure S2), our data suggest that the temperature-induced

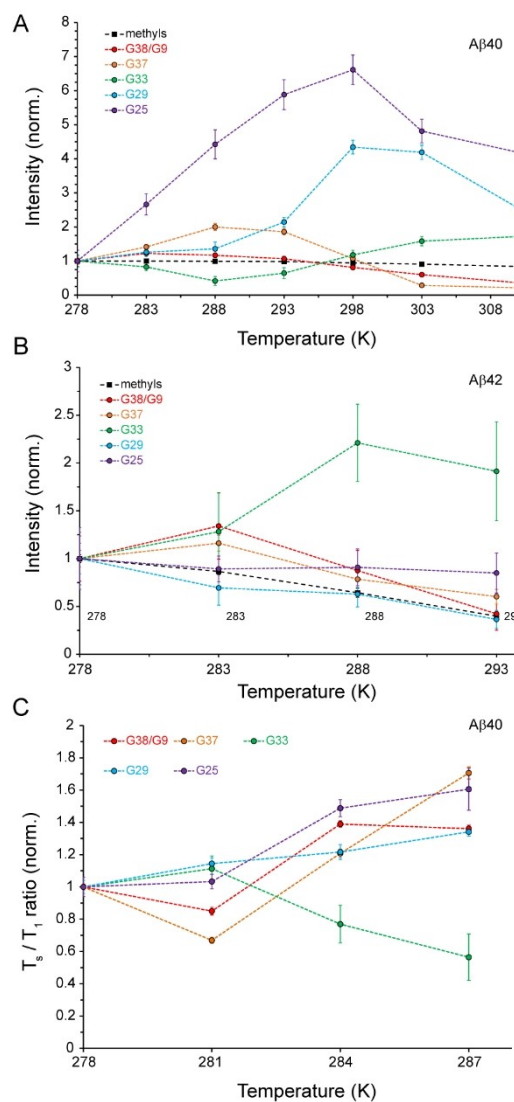


Figure 6. Temperature dependence of glycine-based singlet-states in A β . A, B. Temperature-induced changes in the intensity of different glycine-based singlet-states are shown for A β 40 (A) and A β 42 (B). The signal intensity in the methyl region represents A β monomer level at each temperature. C. The ratio of singlet-state to spin-lattice relaxation times (T_2/T_1) shown for different glycines of A β 40 in dependence of temperature. The T_2/T_1 ratios are normalized with respect to the value observed at 278 K. In all panels A–C, residue G33 exhibits a distinct behavior (see text for details).

conformational changes of A β are predominantly intramolecular.

A β molecules contain small percentage of β -sheet structure already in the monomeric state, in particular at the C-terminus.^[7,26–28] Our results demonstrate the distinctive behavior of residues G33, L34 and M35 of both A β 40 and A β 42 in response to a temperature rise. The G33 residue is part of the GxxxGxxxGxxxG motif of A β (G25–G29–G33–G37), which may be involved in transmembrane oligomerization of A β by forming a glycine zipper.^[29,30] Previous studies have shown that the G33 substitution with alanine or isoleucine diverts A β aggregation toward less-toxic A β oligomers.^[31] Furthermore, the F19–L34 contact is formed at an early stage of A β 40 aggregation,^[32] and

the L34 V mutation of A β promotes A β aggregation.^[33] Besides, the role of M35 residue in A β 40 oligomerization has been detected via ¹⁹F NMR.^[34] Our data are in accord with the previous reports and furthermore suggest that the alterations in the conformational dynamics of the G33-L34-M35 segment constitute an “early” step of A β aggregation. Notably, this region is distinct from the reported “hot spots” of A β involved in seeded A β aggregation,^[25,35] nevertheless the observed oscillation in the peak intensity profile of A β 's C-terminal residues during seeded aggregation is in agreement with the proposed role of the C-terminal region during early A β aggregation.^[35] Furthermore, these residues of A β may play a role in the micelle-like peptide oligomerization, as suggested in,^[36] an arguably key step in the aggregation of A β and other amyloid peptides,^[5,37] and their cross-seeded aggregation.^[38]

In both variants of A β , the C-terminal residues (V40 in A β 40 and A42 in A β 42) appear to be involved in the early steps of aggregation. However, unlike A β 40, the distinct temperature-dependence of side-chain dynamics in the C-terminal region of A β 42 is accompanied by changes in the backbone dynamics of V24-K28 and relative rigidity of M35-G38 (Figure 1B). Besides, previous studies have shown that S26 phosphorylation or phosphomimetic mutation (S26D) induces the formation of a local salt bridge with K28 side chain and increases the mobility of C-terminal residues distal to K28.^[27] This non-native salt bridge was proposed to underlie the observed anti-aggregation effect of S26 phosphorylation.^[27,39] Inspired by these data, we hypothesize that elevated temperature brings the middle and C-terminal regions of A β closer to each other and promotes the formation of a salt bridge between K28 side chain and the C-terminal carboxyl group. As shown in another protein system,^[40] the formation of this salt bridge can be favored at higher temperatures because of the entropic gain originating from desolvation effects. The formation of this long-range salt bridge leads to the relative compaction of A β 42 monomers, consistent with the slight reduction of the R_h of A β 42 at high temperatures. This salt bridge has been observed in recent structural models of A β 42 fibrils,^[9,10] and our data proposes that it may form during the “early” steps of the misfolding of A β 42. It is however notable that the salt-bridge disrupting K28E mutation induces only small differences in the chemical shifts of A30-G37 of A β 42 at 278 K,^[7] indicating that the speculated salt bridge is not present at low temperatures. Further studies are required to test the proposed hypothesis.

Glycine residues are believed to play important roles in controlling protein aggregation and liquid-liquid phase separation.^[41,42] Proteins undergoing neurodegeneration-related aggregation, such as A β and tau protein, α -synuclein and dipeptide repeat (DPR) proteins^[43] contain large numbers of glycines frequently located in the key regions of the protein sequence. In AD, several mutations introduce glycine into A β sequence, which can alter the structure and dynamics of A β fibrils.^[44] In addition, glycine residues of A β are potential players in peptide-lipid membrane interactions.^[45,46] The use of glycine-based singlet-states as exemplified in this study allows site-specific monitoring of conformational changes during aggregation without the need for uniform or selective isotope labeling

of proteins. Unlike amide protons, the use of glycine HAs is not compromised by rapid amide-water exchange rates in disordered proteins. Besides, new insights into the mechanism of peptide aggregation or peptide-membrane interaction can be obtained through dynamical information encoded in the singlet-state relaxation times.^[23]

In summary, we have demonstrated that the C-terminal region of A β plays a distinctive role during the earliest steps of temperature-induced misfolding and aggregation. Our data highlights the plasticity of the aggregation mechanism in A β peptides and defines the C-terminal region as a potential target in the rational design of A β 42 aggregation inhibitors.

Acknowledgements

N.R.-G. acknowledges German Research Foundation (DFG) for research grants RE 3655/2-1 and 3655/2-3. We are grateful to Markus Zweckstetter and Christian Griesinger for useful discussions and Karin Giller for assistance in A β production. Open Access funding enabled and organized by Projekt DEAL.

Conflict of Interest

The authors declare no conflict of interest.

Keywords: amyloid beta-peptides · NMR spectroscopy · singlet-state · aggregation · Alzheimer's disease

- [1] D. J. Selkoe, J. Hardy, *EMBO Mol. Med.* **2016**, *8*, 595–608.
- [2] R. Sengoku, *Neuropathology* **2020**, *40*, 22–29.
- [3] R. Riek, P. Guntert, H. Dobeli, B. Wipf, K. Wuthrich, *Eur. J. Biochem.* **2001**, *268*, 5930–5936.
- [4] J. T. Jarrett, E. P. Berger, P. T. Lansbury Jr., *Ann. N. Y. Acad. Sci.* **1993**, *695*, 144–148.
- [5] G. Bitan, M. D. Kirkitadze, A. Lomakin, S. S. Vollers, G. B. Benedek, D. B. Teplow, *Proc. Natl. Acad. Sci. USA* **2003**, *100*, 330–335.
- [6] Y. L. Yan, C. Y. Wang, *J. Mol. Biol.* **2006**, *364*, 853–862.
- [7] T. Kakeshpour, V. Ramanujam, C. A. Barnes, Y. Shen, J. Ying, A. Bax, *Biophys. Chem.* **2020**, *270*, 106531.
- [8] J. X. Lu, W. Qiang, W. M. Yau, C. D. Schwieters, S. C. Meredith, R. Tycko, *Cell* **2013**, *154*, 1257–1268.
- [9] L. Gremer, D. Scholzel, C. Schenk, E. Reinartz, J. Labahn, R. B. G. Ravelli, M. Tusche, C. Lopez-Iglesias, W. Hoyer, H. Heise, D. Willbold, G. F. Schroder, *Science* **2017**, *358*, 116–119.
- [10] M. T. Colvin, R. Silvers, Q. Z. Ni, T. V. Can, I. Sergeev, M. Rosay, K. J. Donovan, B. Michael, J. Wall, S. Linse, R. G. Griffin, *J. Am. Chem. Soc.* **2016**, *138*, 9663–9674.
- [11] M. A. Walti, F. Ravotti, H. Arai, C. G. Glabe, J. S. Wall, A. Bockmann, P. Guntert, B. H. Meier, R. Riek, *Proc. Natl. Acad. Sci. USA* **2016**, *113*, E4976–4984.
- [12] S. Parthasarathy, M. Inoue, Y. Xiao, Y. Matsumura, Y. Nabeshima, M. Hoshi, Y. Ishii, *J. Am. Chem. Soc.* **2015**, *137*, 6480–6483.
- [13] D. S. Wishart, *Prog. Nucl. Magn. Reson. Spectrosc.* **2011**, *58*, 62–87.
- [14] M. V. Berjanskii, D. S. Wishart, *J. Am. Chem. Soc.* **2005**, *127*, 14970–14971.
- [15] H. Y. Kim, M. K. Cho, D. Riedel, C. O. Fernandez, M. Zweckstetter, *Angew. Chem. Int. Ed.* **2008**, *47*, 5046–5048; *Angew. Chem.* **2008**, *120*, 5124–5126.
- [16] T. M. Sabo, D. Bakhtiari, K. F. Walter, R. L. McFeeters, K. Giller, S. Becker, C. Griesinger, D. Lee, *Protein Sci.* **2012**, *21*, 562–570.
- [17] Y. Yan, J. Liu, S. A. McCallum, D. Yang, C. Wang, *Biochem. Biophys. Res. Commun.* **2007**, *362*, 410–414.

- [18] S. Mamone, N. Rezaei-Ghaleh, F. Opazo, C. Griesinger, S. Gloeggler, *Sci. Adv.* **2020**, *6*, eaaz1955.
- [19] M. H. Levitt, *Annu. Rev. Phys. Chem.* **2012**, *63*, 89–105.
- [20] G. Pileio, *Prog. Nucl. Magn. Reson. Spectrosc.* **2017**, *98–99*, 1–19.
- [21] A. Bornet, P. Ahuja, R. Sarkar, L. Fernandes, S. Hadji, S. Y. Lee, A. Haririnia, D. Fushman, G. Bodenhausen, P. R. Vasos, *ChemPhysChem* **2011**, *12*, 2729–2734.
- [22] L. Fernandes, C. Guerniou, I. Marin-Montesinos, M. Pons, F. Kateb, P. R. Vasos, *Magn. Reson. Chem.* **2013**, *51*, 729–733.
- [23] K. Nagashima, D. K. Rao, G. Pages, S. S. Velan, P. W. Kuchel, *J. Biomol. NMR.* **2014**, *59*, 31–41.
- [24] N. Rezaei-Ghaleh, G. Parigi, M. Zweckstetter, *J. Phys. Chem. Lett.* **2019**, *10*, 3369–3375.
- [25] N. L. Fawzi, J. Ying, R. Ghirlando, D. A. Torchia, G. M. Clore, *Nature* **2011**, *480*, 268–272.
- [26] J. Danielsson, A. Andersson, J. Jarvet, A. Graslund, *Magn. Reson. Chem.* **2006**, *44 Spec No*, S114–121.
- [27] N. Rezaei-Ghaleh, M. Amininasab, K. Giller, S. Kumar, A. Stundl, A. Schneider, S. Becker, J. Walter, M. Zweckstetter, *J. Am. Chem. Soc.* **2014**, *136*, 4913–4919.
- [28] M. A. Walti, J. Orts, B. Vogeli, S. Campioni, R. Riek, *ChemBioChem* **2015**, *16*, 659–669.
- [29] S. Kim, T. J. Jeon, A. Oberai, D. Yang, J. J. Schmidt, J. U. Bowie, *Proc. Natl. Acad. Sci. USA* **2005**, *102*, 14278–14283.
- [30] W. Liu, E. Crocker, W. Zhang, J. I. Elliott, B. Luy, H. Li, S. Aimoto, S. O. Smith, *Biochemistry* **2005**, *44*, 3591–3597.
- [31] A. Harmeier, C. Wozny, B. R. Rost, L. M. Munter, H. Hua, O. Georgiev, M. Beyermann, P. W. Hildebrand, C. Weise, W. Schaffner, D. Schmitz, G. Multhaup, *J. Neurosci.* **2009**, *29*, 7582–7590.
- [32] J. Adler, H. A. Scheidt, M. Kruger, L. Thomas, D. Huster, *Phys. Chem. Chem. Phys.* **2014**, *16*, 7461–7471.
- [33] A. Hatami, S. Monjazebe, S. Milton, C. G. Glabe, *J. Biol. Chem.* **2017**, *292*, 3172–3185.
- [34] Y. Suzuki, J. R. Brender, M. T. Soper, J. Krishnamoorthy, Y. Zhou, B. T. Ruotolo, N. A. Kotov, A. Ramamoorthy, E. N. Marsh, *Biochemistry* **2013**, *52*, 1903–1912.
- [35] J. R. Brender, A. Ghosh, S. A. Kotler, J. Krishnamoorthy, S. Bera, V. Morris, T. B. Sil, K. Garai, B. Reif, A. Bhunia, A. Ramamoorthy, *Chem. Commun.* **2019**, *55*, 4483–4486.
- [36] B. R. Sahoo, S. J. Cox, A. Ramamoorthy, *Chem. Commun.* **2020**, *56*, 4627–4639.
- [37] J. R. Brender, J. Krishnamoorthy, M. F. Sciacca, S. Vivekanandan, L. D'Urso, J. Chen, C. La Rosa, A. Ramamoorthy, *J. Phys. Chem. B* **2015**, *119*, 2886–2896.
- [38] M. I. Ivanova, Y. Lin, Y. H. Lee, J. Zheng, A. Ramamoorthy, *Biophys. Chem.* **2021**, *269*, 106507.
- [39] N. G. Milton, *NeuroReport* **2001**, *12*, 3839–3844.
- [40] N. Zhang, Y. Wang, L. An, X. Song, Q. Huang, Z. Liu, L. Yao, *Angew. Chem. Int. Ed.* **2017**, *56*, 7601–7604; *Angew. Chem.* **2017**, *129*, 7709–7712.
- [41] C. Parrini, N. Taddei, M. Ramazzotti, D. Degl'Innocenti, G. Ramponi, C. M. Dobson, F. Chiti, *Structure* **2005**, *13*, 1143–1151.
- [42] J. Wang, J. M. Choi, A. S. Holehouse, H. O. Lee, X. Zhang, M. Jahnel, S. Maharana, R. Lemaitre, A. Pozniakovsky, D. Drechsel, I. Poser, R. V. Pappu, S. Alberti, A. A. Hyman, *Cell* **2018**, *174*, 688–699.
- [43] K. Mori, S. M. Weng, T. Arzberger, S. May, K. Rentzsch, E. Kremmer, B. Schmid, H. A. Kretschmar, M. Cruts, C. Van Broeckhoven, C. Haass, D. Edbauer, *Science* **2013**, *339*, 1335–1338.
- [44] M. R. Elkins, T. Wang, M. Nick, H. Jo, T. Lemmin, S. B. Prusiner, W. F. DeGrado, J. Stohr, M. Hong, *J. Am. Chem. Soc.* **2016**, *138*, 9840–9852.
- [45] S. A. Kotler, P. Walsh, J. R. Brender, A. Ramamoorthy, *Chem. Soc. Rev.* **2014**, *43*, 6692–6700.
- [46] M. F. Sciacca, S. A. Kotler, J. R. Brender, J. Chen, D. K. Lee, A. Ramamoorthy, *Biophys. J.* **2012**, *103*, 702–710.

Manuscript received: July 19, 2021

Revised manuscript received: August 5, 2021

Accepted manuscript online: August 6, 2021

Version of record online: August 19, 2021